Research Submitted to the Harvey Mudd College Center for Environmental Studies

Improving Wind Turbine Efficiency through Whales-inspired Blade Design

Prepared By:

Alex Krause

Raquel Robinson

Faculty Advisors:

Professor Hoi Dick Ng, Concordia University

Professor Lori Bassman, Harvey Mudd College

October 5th, 2009

Abstract

Due to the rapid depletion of hydrocarbon-based energy resources and their harmful effects on the environment, there is an urgent need to seek alternative and sustainable energy sources. Wind power is among the potential alternatives to fossil fuels; however, the efficiency to convert wind energy into a useful form such as electricity using wind turbines still requires some engineering design innovation. Energy efficiency in traditional horizontal-axis wind turbine (HAWT) is largely determined by the aerodynamics of the turbine blades and the characteristics of the turbulent fluid flow. The objective of this project is thus to investigate improvement of HAWT blade design by incorporating the bumps on humpback whales' fins into blades. This application is thought to produce more aerodynamic blades by creating turbulence in the airflow behind each groove. This project focused on designing, simulating, and analyzing a HAWT with whale-inspired blades to determine the differences in the associated turbulent flow field, boundary layer attachment, and pressure gradients that cause lift and drag compared to traditional HAWTs using computational studies. It is shown that a whale-inspired blade offers the possibility of an improved design at higher angles of attack. The blade is characterized by a superior lift/drag ratio due to greater boundary layer attachment from vortices energizing the boundary layer.

Background

Wind power is one potential alternative to fossil fuels currently being globally utilized. However, the need to more efficiently convert wind energy into a useful form still requires engineering innovation. Horizontal-axis wind turbines typically utilize traditional airfoil design, with the leading edges as smooth as possible. The resulting low friction serves to minimize turbulent flow around the top of the airfoil. This traditional design has been the HAWT standard for decades but there is new research that suggests a more-efficient design. Humpback whales, an endangered species, possess evolutionary aerodynamic advantages that are just now being understood. The bumps on their fins' leading edges create downwind turbulence. This reduces stalling by keeping layers of flow attached to the top of the airfoil at higher angles of attack. Airfoil stalling occurs once the angle of attack surpasses the critical angle of attack. The separated, turbulent flow, which increases with drag at higher angles of attack, is dominant over the attached flow. This results in a decrease in lift. Initial research suggests, "turbines fitted with tubercles to the leading edges of each blade are able to produce more power at low fluid speeds, are quieter, and perform much better in turbulent fluid streams" [1]. With whale-inspired turbine blades, protrusions/bumps placed on an airfoil act as vortex generators. The vortices cause an increase in inertia of the boundary layer airflow separation which results in a delay in stall. It is possible that at high angles of attack, these vortex generators can be used to reattach flow, increasing lift.

Introduction

Traditional combustion-based energy sources have had an increasing negative impact worldwide, both environmentally and economically. Consequently, the demand for clean, low-cost and renewable energy sources is at an all time high in today's society. One such energy source is wind energy, an environmentally friendly and renewable alternative, based on a resource that is essentially free and limitless. Wind energy has already proven itself as a viable resource in Western European countries. However, further development in several areas of wind energy technology is needed, especially in the area of blade design. Improved aerodynamics of blades is likely to yield not only more extracted energy, but lower costs as well.

Research in whale-inspired blade design has already proven very promising. Comparative studies have shown that the power output from whale-inspired blades is higher than that of traditional blades. For example, a study by the Wind Energy Institute of Canada compared experimentally Wenvor (traditional) blades and Whalepower blades. It concluded that though both had the same startup wind speed of 5 m/s, the Whalepower blades had a greater power curve and reached rated power at a lower speed than the Wenvor blades [2].

Modeling Methodology

Modeling the blade designs was done through use of computer aided design (CAD). An assembly was created in order to incorporate the blade, control volume, and angle of attack. The assembly was then imported into a computational fluid dynamics package in order to simulate flow over the blade models.

Blade Modeling

Pro/ENGINEER is a professional 3D CAD software package, which can be used to generate representative models of blade design. The design for a standard airfoil was created using the blend function included in the software. Cross sections, at specific points along the length of the blade (per the blade carving tutorial found on the Scoraig Wind Electric website [3]), were created and blended together to give the blade a smooth finish (Figures 1-3). The blade is 1150mm in length. From its tip to root, the blade tapers in thickness along the leading edge. The thickness increases from 11mm at the tip to 25mm at the beginning of the root section. The root section has a constant thickness of 50mm.

The blade's width also increases gradually from tip (90mm) to root (150mm). Additionally, in order to optimize the angle of attack all along the blade, it twists from root to tip. The two edges of the root section are chamfered leaving a 120 degree angled base. This allows for a three blade assembly. A regular repeating bump pattern was created by creating an area of material removal using arcs and lines and extruding the material removal through the blade. In the horizontal bumped blade, the area of material removal was made on top of the blade and extruded vertically through the leading edge of the blade (Figure 4). In the vertical bumped blade, the area of material removal was made on the face of the leading edge and extruded horizontally into the blade.

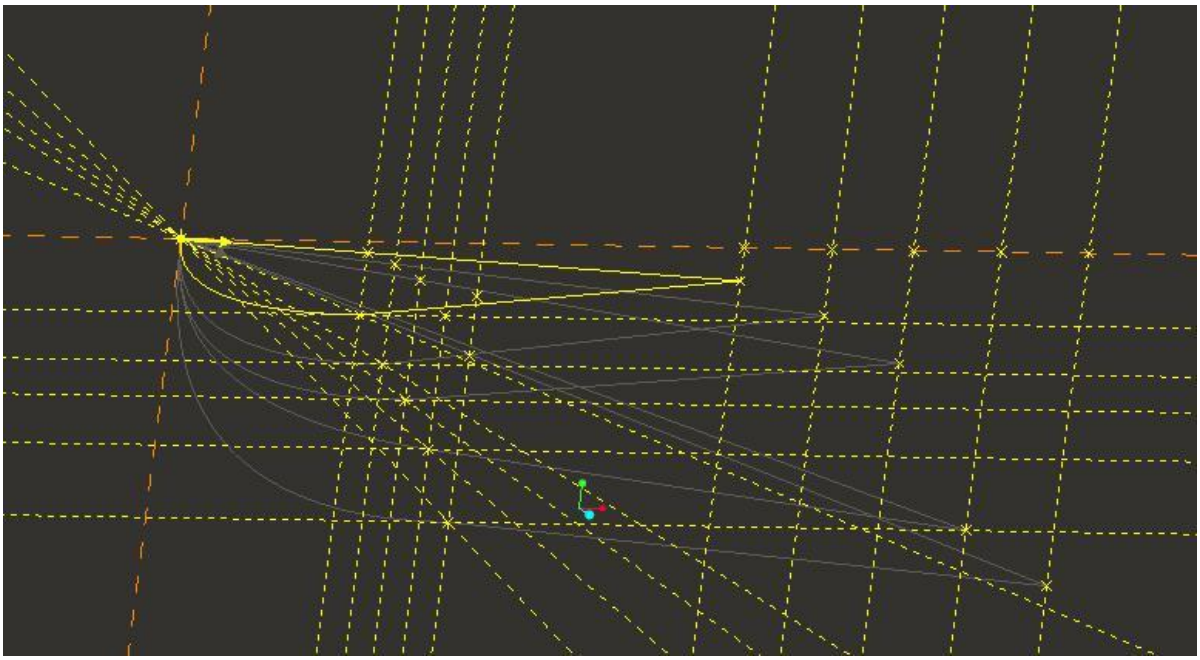

Figure 1. Illustrating airfoil cross-sections use to create a smooth blend.

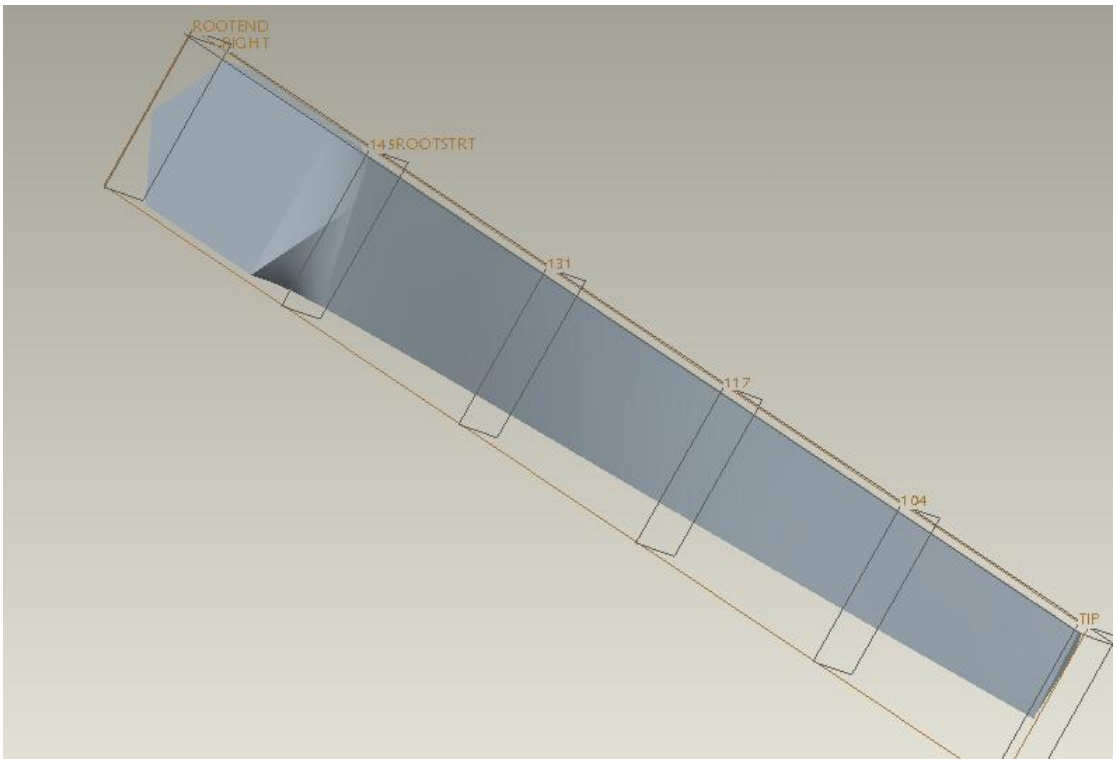

Figure 2. Completed unbumped blade (front view).

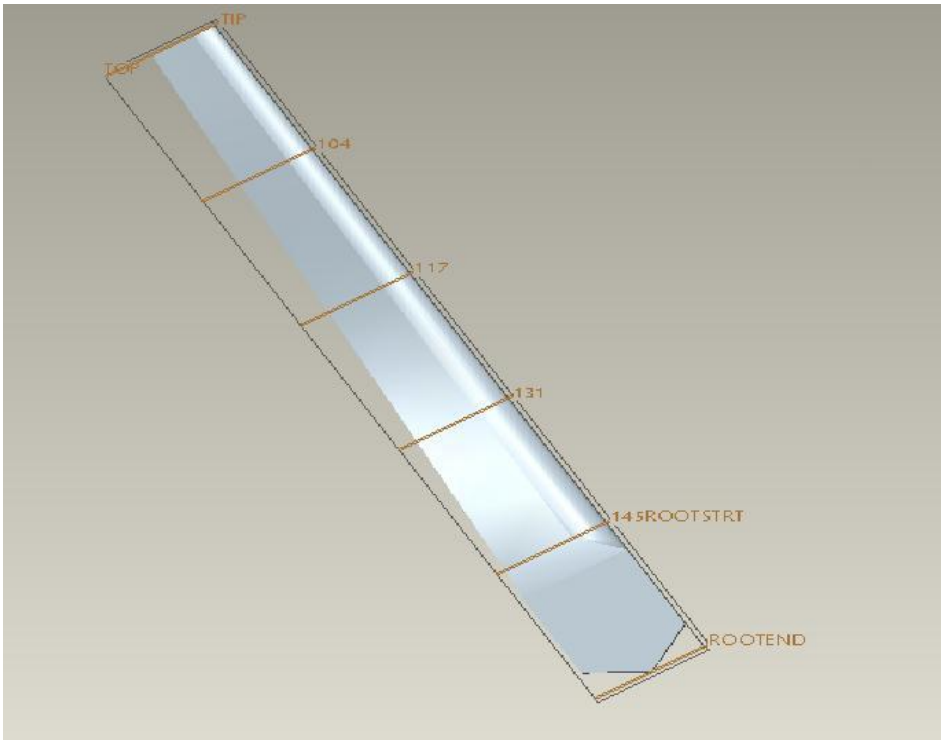

Figure 3. Completed unbumped blade (rear view).

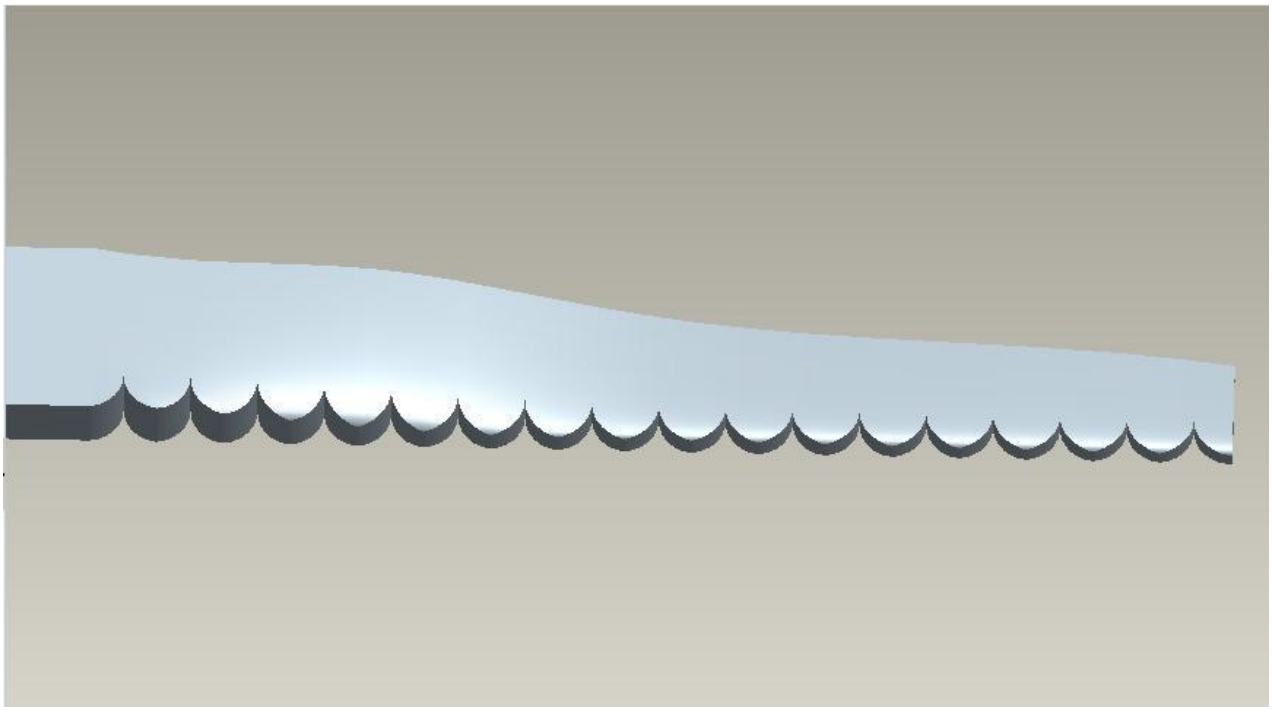

Figure 4. Completed horizontal bumped blade design (rear view).

In order to integrate the Pro/ENGINEER models into CFdesign, an assembly model had to be made in Pro/ENGINEER. Increasing the AoA of the blades requires rotating the blade with respect to CFdesign's control volume. CFdesign has no built-in functionality to rotate the blade for a specified AoA. Therefore an assembly was made in Pro/ENGINEER in which the control volume was made out of a 3D shell, which is automatically recognized by CFdesign. The blade was placed within the shell and mated such that it was located in the necessary position, as described in the following section. The angle of attack is set by creating an angled datum plane mated to the leading edge of the blade, causing the leading edge of the blade to be angled away from the inlet flow. The control volume assemblies were then imported into CFdesign, which offers a computational simulation of flow over the blade.

Blade Simulation

CFdesign is used to numerically study the flow field over different blade designs. While CFdesign is not quantitatively accurate for modeling wind turbine flow, it is qualitatively useful for seeing how bumps alter airflow over the blades. CFdesign is able to

import blade designs created in Pro/ENGINEER. In order to decrease processing time, only a portion of each blade, one-fifth of the blade length, was simulated. An adequate control volume created in the Pro/ENGINEER assembly for the simulation has a length ten times the blade's length. The height is sixty times the blade's height, and the depth is two hundred times the blade's depth. The blade is placed in the center of the width and height of the control volume, but is placed near the front face to allow greater space for the wake. The blade is set in the traditional airfoil orientation, such that the inlet flow is into the leading edge. This orientation is selected for the first round of CFdesign testing because of provided insight into the effect of the bumps on the flow field. The imported assembly can be seen in Figure 5 below.

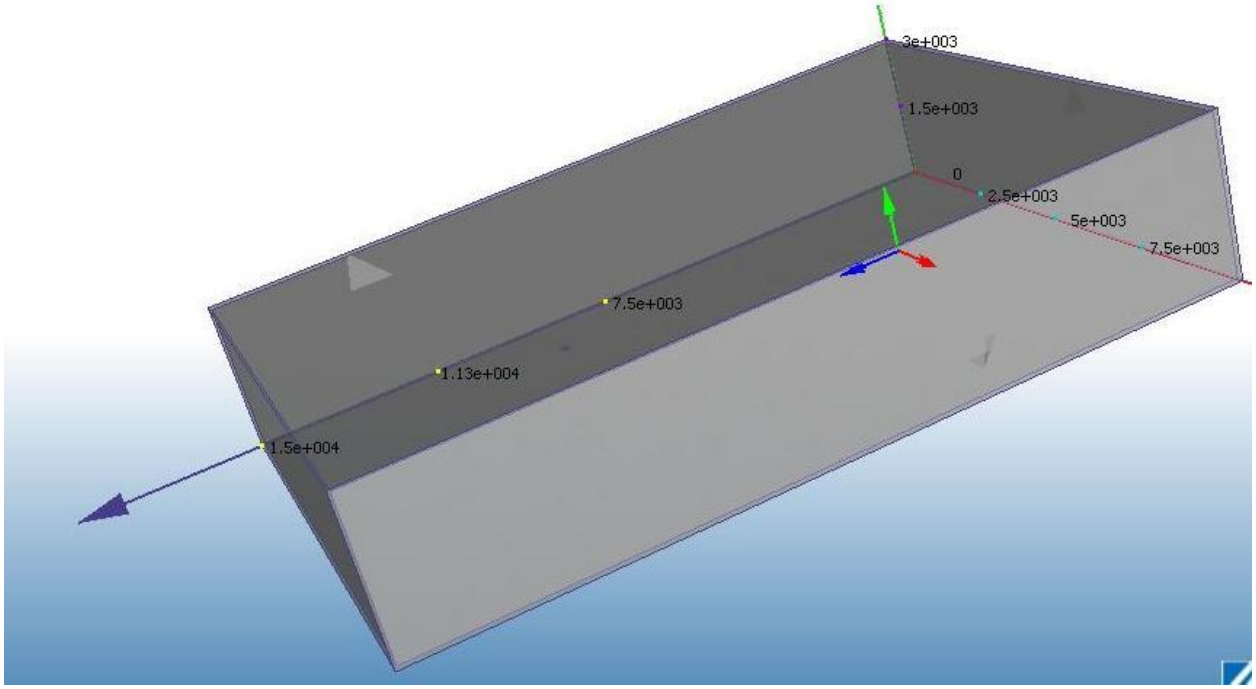

Figure 5. Imported control volume assembly in CFdesign. Blade section is the small dark-grey dot in between 1.13e+004 and 7.5e+003 along the blue arrow.

The boundary conditions for the control volume surfaces are set to mimic wind tunnel behavior. The inlet has a velocity of 4,000 mm/s, the outlet has zero gauge pressure, and the four other surfaces all have slip/symmetry. CFdesign allows for initial conditions, but this simulation requires none. CFdesign discretizes the fluid in the control volume using a mesh made up of finite elements. Automatic mesh sizing is used with additional mesh refinement around the blade. When the part is imported into CFdesign, the semicircular bumps become linearized. Since it is essential to retain the bumps' original

shape, the mesh must be very dense around the leading edge. Mesh must also be dense in the wake in order to improve the accuracy of determining the flow attachment. A mesh refinement region was created to encapsulate these areas (Figure 6). Mesh density in the refinement regions was increased until numerical results were independent of the mesh density. The fluid material is set as air at STP while the blade material is set as solid aluminum. Since heat transfer is being ignored, the material of the blade has marginal effect on the flow field as long as it is solid. Motion was not necessary for static blade testing, but could be utilized in additional studies.

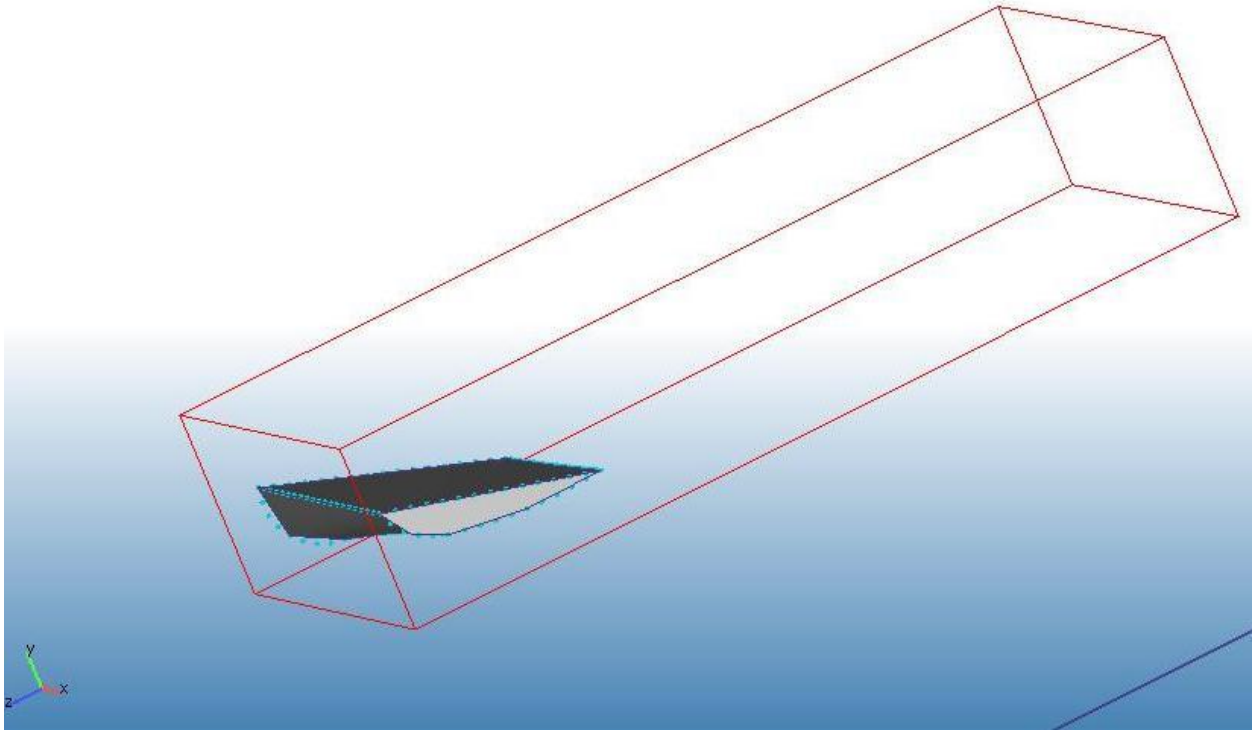

Figure 6. Control blade section with mesh refinement region depicted as rectangular prism.

Turbulence adheres to the k-epsilon model, with a constant Tub/Lam ratio of 10 and a turbulence intensity of 0.1. Solution control was also utilized in order to ensure numerical convergence. Once the numerical solutions converged, the simulation was terminated. The number of maximum iterations was set to 1,000, with solution control ending the simulation typically around 200-600 iterations. CFdesign has an extensive analysis functionality that was utilized to analyze the results of the simulations (Figure 7).

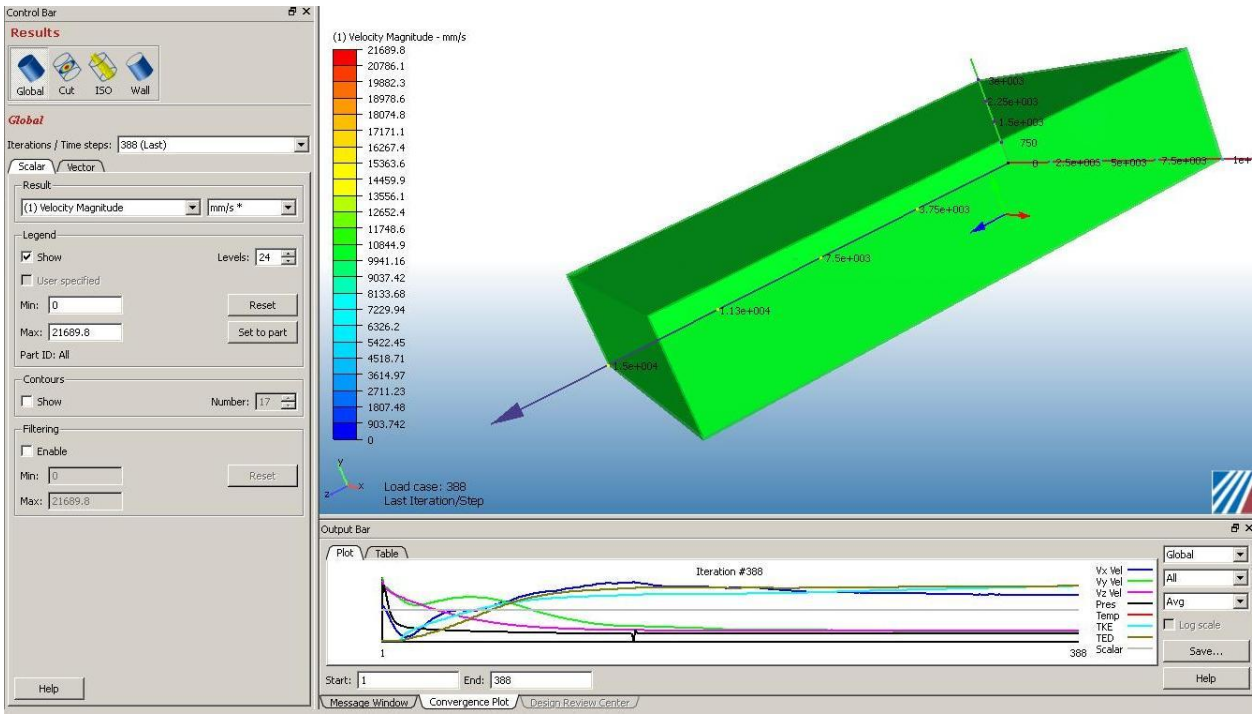

Figure 7. CFdesign result window. Convergence plot on the bottom indicates numerical convergence. Panel on the left provides analysis capabilities.

Analysis Methodology

Comparison of the three blade designs was achieved by investigating three parameters: streamlines, lift/drag, and pressure coefficients. Streamlines provided a visualization of the path of air particles over the blades. From this, vortices, turbulence, and flow attachment could be visually observed. Lift/drag provided an important quantitative comparison in the lift and drag provided by the pressure difference across each blade. The pressure coefficient provides similar insight as lift and drag, with the added benefit of providing localized data.

Streamlines

Fluid flow is either laminar or turbulent. In laminar (streamlined) flow, the fluid progresses with the same speed in all directions. On the other hand, turbulent flow is chaotic and unpredictable. It is made up of circular currents of air that push on a surface in unexpected ways. Almost all fluid flow demonstrates some degree of turbulent flow. The layer of fluid in the immediate vicinity of the airfoil surface is known as the boundary layer.

The more turbulent the flow, quantitatively characterized by turbulent kinetic energy (TKE), the more turbulent the boundary layer.

Flow is often analyzed through a 3D flow velocity vector field. Streamlines are instantaneously tangent to these velocity vectors within the 3D field. Since there cannot be two different velocities at the same point, streamlines cannot intersect each other or themselves. Pathlines are the trajectories that a single particle takes within the field. In general, pathlines can intersect each other or themselves. The only points within a pathline that are indefinitely unique are the start and end of the particle's path. With steady flow, as used in the CFdesign simulations, pathlines and streamlines are equivalent (and therefore will be discussed interchangeably) because the time derivative terms are zero. Consequently, for the steady flow used, the pathlines cannot intersect each other or themselves.

Streamlines/pathlines are useful as visualizations of flow within CFdesign simulations. CFdesign allows for a trace of selected points at the front of the flow volume. Points traced along the top of the leading edge can depict whether or not vortices have formed behind the bumps of the experimental blades. A recirculating streamline, explicit in CFdesign, indicates a vortex. Vortices indicate that the experimental design is successful in energizing the boundary layer, potentially keeping downstream flow attached to the blade. Additionally, streamlines can be used to display the flow over the top of the blade. When the streamlines are pulled closer to the top of the blade, the flow is more attached. More attached flow will decrease pressure on top of the blade, producing more lift, which can ultimately improve the efficiency of the blade in a turbine setup.

Lift and Drag

Experimentally, it is clear that a flow moving around an airfoil exerts a force on the airfoil. This observation can be explained in multiple ways using varying principles. The most palpable explanation employs Newton's laws. Upon passing around the airfoil, the upstream flow is deflected downwards farther downstream. This change in direction of flow implies a force acting on the flow, which, by Newton's third law, implies an equal and opposite reaction force acting on the airfoil. A more rigorous explanation can be obtained by considering two streamtubes, one above and one below the stagnation streamline. The upper streamtube is compressed relative to the lower streamtube due to the geometry and angle of attack of the airfoil. Conservation of mass then implies that the flow velocity in the upper streamtube is greater than that of the lower. From Bernoulli's principle it directly

follows that the faster velocity of flow over the top of the airfoil creates a region of lower pressure above the airfoil. The pressure difference results in an aerodynamic force.

This aerodynamic force can be standardized into two component forces: lift and drag. Drag is the component of the aerodynamic force that acts parallel to the incident flow, while lift is the component that acts perpendicular to the incident flow. The geometry of wind turbine blades is such that lift is always oriented in the upward direction. Lift and drag are two significant variables that can indicate the quality of the aerodynamics of a blade design. By increasing lift and decreasing drag on blades, overall efficiency of the turbine can be improved. Lift and drag of various blade designs can be compared at differing angles of attack (AoA), serving as indicators of the effectiveness of the bumped blade designs. Increase in the AoA up to the critical angle results in an increase in both lift and drag. Alternatively, further increase in angle of attack beyond the critical angle yields a decrease in lift and a substantial increase in drag.

Comparing drag and lift forces across differently-sized blades necessitates the use of dimensionless coefficients of lift and drag. The drag coefficient normalizes drag force by the mass density of the field, *p*, free stream velocity, *v*, and planform area, *A*:

$$C_d = \frac{2F_d}{pv^2A}. \qquad (1)$$

The lift coefficient is found in a similar fashion:

$$C_l = \frac{2F_l}{pv^2A}. \qquad (2)$$

Since density of the field (air) and free stream velocity were kept constant throughout all trials, the drag and lift coefficients effectively allow comparing of drag and lift normalized by planform area. Planform area for the blades was found using the top surface.

Pressure Coefficient

An examination of the coefficient of pressure is one of the simplest and most commonly used ways to analyze the aerodynamic performance of airfoil sections. Consideration of the coefficient of pressure can give one a sense of the resultant forces acting on the airfoil. The coefficient of pressure, *Cp*, describes the relative pressure throughout a flow field. It is the difference between local static pressure non-dimensionalized by freestream dynamic pressure. It is calculated by the following equation:

$$C_p = \frac{2(p - p_\infty)}{\rho_\infty {V_\infty}^2}. \qquad (3)$$

Where p is the pressure at the point of evaluation, $p\infty$ is the pressure in the freestream, $\rho\infty$ is the freestream fluid density, and $v\infty$ is the freestream fluid velocity.

Ideally for a typical airfoil, the C_p should start from about 1.0 at the stagnation point, the point on the leading edge where the velocity is zero, rise rapidly on both upper and lower surfaces, and then recover to a small positive value near the trailing edge. The pressure at the trailing edge is related to the airfoil thickness and shape. For thick airfoils the pressure of the trailing edge is slightly positive (the velocity is a bit less than the freestream velocity). For infinitely thin sections, C_p is zero at the trailing edge. Large positive values of C_p at the trailing edge imply more severe adverse pressure gradients. The coefficient for the upper surface is usually well below zero, while that of the lower surface is usually positive. This is due to the fact that the velocity on the underside of the airfoil is less than that of the freestream velocity. The absolute difference between the coefficients of the upper and lower side of the airfoil can give an indication of aerodynamic efficiency of the blade.

Results

The CFdesign simulations were analyzed using the built-in CFdesign analysis functionality. Streamlines around the blade, lift and drag, and pressure coefficients are compared.

Streamlines

At a 0° AoA, as expected, pathlines over the control blade indicate laminar flow that is attached to the blade's surface. The two bumped blades both have distinct vortices forming behind the bumps. The horizontal bumped blade's vortices are larger than the vertical bumped blade's vortices, which suggests a more energized and turbulent boundary layer. At a 10° AoA, the control blade has a substantial amount of recirculation behind the blade and the flow is reattached significantly far downstream. The horizontal bumped blade exhibits recirculation as well, but less than that of the control blade. Flow reattaches at a closer distance downstream of the horizontal blade than with the control blade. The vertical bumped blade has much less recirculation than both other blades, with more laminar flow attached at a closer distance. It is difficult to discern between the recirculation caused exclusively by the bumps and that caused by the overall airfoil shape (such as with the control blade) at a nonzero AoA. At 20° AoA, the blades exhibit the same pattern, with

greatest flow attachment in the vertical bumped blade, followed by the horizontal bumped blade, and finally the control blade.

Lift and Drag

As expected, C_d increases with increasing AoA for the control (non-bumped) blade (Figure 5). C_l also increases with greater AoA, suggesting that the critical angle might be beyond 20°. These trends are exhibited with the two bumped blades as well, except for an aberrant C_d value for the vertically bumped blade at 20° AoA. Upon increase of AoA, the horizontal bumps blade has an increasingly comparable C_l and a progressively lower C_d compared to the control blade. Thus the C_l to C_d ratio for the horizontal bump blade is increasingly better than the C_l to C_d ratio for the control blade with increasing AoA. This relationship suggests that at higher AoAs, the horizontal bump blade is more aerodynamic than the control. The vertical bumps blade experiences marginal gains in C_l with increasing AoA compared to the steady increases in C_l for the control blade. The increase in C_d at 10° AoA followed by the decrease at 20° AoA, which defies the conventional relationship between C_d and AoA, yields an increase in the C_l to C_d ratio even though there is marginally more lift. Overall, the vertical bump blade offers an improved C_l to C_d ratio compared to the control blade, but inferior ratios compared to the horizontal bumps blade.

	Control – No Bumps			**Horizontal Bumps**			**Vertical Bumps**		
AoA (°)	**C_l**	**C_d**	**C_l/C_d**	**C_l**	**C_d**	**C_l/C_d**	**C_l**	**C_d**	**C_l/C_d**
0	0.263	0.226	1.164	0.187	0.137	1.365	0.172	0.123	1.398
10	0.364	0.27	1.348	0.319	0.172	1.855	0.218	0.156	1.397
20	0.447	0.28	1.596	0.438	0.207	2.116	0.223	0.115	1.939

Figure 8. Quantitative comparison of lift and drag coefficients.

Pressure Coefficient

All airfoil designs tested exhibit a coefficient of pressure along the leading edge of approximately one. As expected the *ΔCp* value for the control blade increases with an increase in AoA from 0° to 10°. This was followed by a decrease from 10° to 20° which suggested that past 10° the critical angle was exceeded. At an AoA of 0°, the coefficient of the trailing edge of the upper surface was slightly positive, indicating a thick airfoil shape.

For the horizontal bumped blade design an increase in aerodynamic efficient was not evident. At 0°, the upper side had a negative average value, but with positive values near the trailing edge. On the underside, the value was positive with no noted decrease in value towards the trailing edge as was observed with the unbumped design. The *ΔCp* was greater than that of the control. At 10° the value on the upper side of the airfoil was more negative than at 0°. On the underside the value remain below zero. This yielded an unexpected decrease in the *ΔCp*. At 20°, the results were more promising with a substantial increase in *ΔCp* in the horizontal bumped blade compared to the control.

The vertical bumped blade yields results similar to that of the control blade, except for at 20° AoA. The *ΔCp* value increases with an increase in AoA from 0° to 10° and fell as AoA went from 10 to 20 degrees. At 0°, the difference between pressure coefficient on the upper and lower sides was minimal. The value obtained at twenty degrees, suggests that the critical angle had likely been exceeded. A consideration of coefficient of pressure gives inconclusive results as to which blade design is superior.

	ΔC_p		
AoA (°)	**Control – No Bumps**	**Horizontal Bumps**	**Vertical Bumps**
0	0.217	0.351	0.262
10	0.644	0.283	0.613
20	0.353	0.586	0.115

Figure 9. Quantitative comparison of C_p.

Conclusions and Recommendations

The horizontal bump blade holds promise at a high AoA due to its improvement in the lift/drag ratio caused by indicated vortex formation behind the bumps. Streamlines imply a more attached boundary layer near the trailing edge of the blade. The coefficient of pressure gradient indicates that at 20° AoA the horizontal bumps blade was achieving a greater pressure difference than the control and vertical bumps blade. The vertical bumped blade showed potential from a design standpoint, but has inconsistent and discouraging results upon simulation.

In order to better understand the relationship between bumps and aerodynamic efficiency, additional bump designs should be considered. New bump designs could vary relative size of bumps to the blades, the shape of the bumps, and the axis on which the bumps are extruded. A shortcoming of this research was that models were based on one

initial design which is not used in large-scale wind turbine setups. Future studies should utilize multiple, widely used, initial blade designs. The relationship between the efficiency of an individual blade and the overall assembly setup efficiency was never established. Future research should identify aerodynamics parameters in turbine assembly setup testing. Furthermore, the analytical models should be verified through empirical testing with a full assembly setup.

References

[1] Blain, Loz. "Bumpy whale fins set to spark a revolution in aerodynamics." Gizmag 20 March 2008. <http://www.gizmag.com/bumpy-whale-fins-set-to-spark-a-revolution-in-aerodynamics/9020/>

[2] Howle, Laurens E. "Whalepower Wenvor Blade: A report on the efficiency of a whalepower corp. 5 meter prototype wind turbine blade." 24 January 2009. <http://www.whalepower.com/drupal/files/PDFs/Dr_Lauren_Howles_Analysis_of_WEICan_Report.pdf>

[3] Piggott, Hughs. "Carving Wooden Blades." Scoraig Wind Electric. < http://www.scoraigwind.com/selfblade/index.htm >

Appendix A

University of Western Ontario Experiment

The University of Western Ontario's Wind Engineering Group is a worldwide leader in wind engineering research. Since 1965, its Boundary Layer Wind Tunnel Laboratory (BLWTL) has been used by engineers and architects from all over the world to study the effects of wind on countless buildings and bridges. Studying the effects of wind on scale models of these structures allows for improvement and optimization of the design. Often these structures are tested with models of the surrounding buildings because of the significance of the other buildings' effect on wind flow. Noteworthy buildings tested include the World Trade Center, Sears Tower, and CN Tower. Furthermore, researchers have utilized the laboratory to study computational wind engineering and environmental issues. The laboratory allows for studying of a wide array of challenging topics that require simulation of the Earth's wind boundary layer. Cutting-edge topics such as "wind-driven rain impact on buildings," pedestrian-level wind, and wind turbine design are studied (Alan G. Davenport Wind Energy Group).

There are two wind tunnel facilities at the BLWTL: the BLWT 1 and the BLWT2. The BLWT1 was built first, in 1965, and is an open-loop design. The larger BLWT2, which was used in this experiment, was constructed in 1984. The tunnel is a closed-loop design with two long parallel straight-aways. The wind turbine setup has three main components: the high speed test section, the low speed test section, and the water channel wave tank. The turbine is connected to the inlet of the low speed test section. The low speed test section has dimensions of 52m x 5m x 4m (length x width x height) and a maximum free stream velocity of 36 km/hr. This section is used for "full aeroelastic studies of long span bridges, the dispersion of pollutants, rain and snow studies" and is the section best suited for the testing of wind turbines (Alan G. Davenport Wind Energy Group). A wave tank situated below the floor paneling of the low speed test section allows for study of the effect of wind and wind-induced waves on ships or offshore platforms. The wave tank runs the entire length of the low speed test section and is 2m deep. The outlet of the low speed test section is redirected 180° to the inlet of the high speed test section. The pathway is compressed, which, by conservation of mass, increases free stream velocity. The high speed test section has dimensions of 39m x 3.4m x 2.5m and a maximum free stream

velocity of 100 km/hr. This section allows for study of "aeroelastic behavior and pressures on buildings and other structures" and also the effects of wind on towers and bridges (Alan G. Davenport Wind Energy Group). The outlet of the high speed test section connects to the turbine inlet and completes the circuit. Rotating discs in both the low and high speed sections allow for rotation of the model structure or landscape. This allows for testing of different angles of incident wind in real time.

In Mid-July, the research team visited the UWO wind tunnel to observe and help with the setup of an experiment being conducted by the graduate student on our research team. A common concern surrounding wind energy technology is the downwind impact that turbines have on the environment. Consequently, much research is conducted to further understand the behavior of the wake, the long trail of turbulent and slow moving wind behind a wind turbine. The objective of this experiment was to observe the correlation, if any, between wake behavior and the size of rotor and post. This experiment involved blades of three different sizes. The blade chord length, rotor diameter and post diameter were scaled appropriately to maintain consistency between results. The experiment utilized Particle Image Velocimetry (PIV). PIV is an optical method for fluid visualization. Using this technology, one can obtain streamline images and the instantaneous velocity of any region in a flowing fluid field. The fluid, air, is seeded with trace particles. The motion of these particles is captured by a high speed camera. All PIV images were captured in the horizontal plane. The behavior was observed in two locations: behind the post and rotor and behind the rotor only. The camera takes two snapshots milliseconds apart. These images are used to calculate streamlines, the velocities at various points in the wake.